

Giant thermopower changes related to the resistivity maximum and colossal magnetoresistance in EuCd_2P_2

Judith Grafenhorst

Technische Universität Dresden, 01062 Dresden, Germany

Sarah Krebber, Kristin Kliemt, and Cornelius Krellner

*Kristall- und Materiallabor, Physikalisches Institut,
Goethe-Universität Frankfurt, 60438 Frankfurt/M, Germany*

Elena Hassinger

*Institute for Quantum Materials and Technologies,
Karlsruhe Institute of Technology, 76131 Karlsruhe, Germany
Technische Universität Dresden, 01062 Dresden, Germany and
Max Planck Institute for Chemical Physics of Solids, 01187 Dresden, Germany*

Ulrike Stockert*

*Technische Universität Dresden, 01062 Dresden, Germany
Max Planck Institute for Chemical Physics of Solids, 01187 Dresden, Germany and
Institute for Quantum Materials and Technologies,
Karlsruhe Institute of Technology, 76131 Karlsruhe, Germany*

* correspondence should be addressed to ulrike.stockert@tu-dresden.de

(Dated: February 11, 2026)

Abstract

We present the thermopower of EuCd_2P_2 , a material which exhibits a large resistivity peak with significant magnetic field dependence in the temperature range of 10-25 K. In the same region we observe a highly unusual behavior of the thermopower with two sign changes and giant extrema. The overall variation of the thermopower exceeds 4 000 $\mu\text{V/K}$ and takes place in an extremely narrow temperature region of less than 5 K. The anomaly is suppressed completely in a small magnetic field of 0.5 T. We discuss this observation using a simple drift-diffusion picture and taking into account that the temperature gradient inducing the thermopower voltage is accompanied by a gradient of the electrical resistivity. Our simple estimation yields the correct magnitude, shape, and field dependence of the thermopower anomaly observed in EuCd_2P_2 . These results open a new route to giant thermopower values via gradients of electronic properties.

Thermoelectric materials have a large potential for applications based on the conversion of thermal to electrical energy and reverse [1]. The efficiency of these processes is determined by the thermoelectric figure of merit $zT = \sigma S^2 T / \kappa$, which depends on the electrical and thermal conductivities σ and κ , the thermopower S , and temperature T . A high zT and therefore also a large S is a prerequisite for profitable thermoelectric cooling and appreciable enhancement of the overall power efficiency of technical processes by using waste heat for voltage generation. Beyond that, materials with a large thermopower could be used in thermocouple sensors. A strong field dependence of $S(T)$ would even allow to design thermoelectric devices and sensors controlled by magnetic fields [2]. This motivates the exploration of preconditions and mechanisms allowing for large thermopower values and changes.

The thermopower S of conventional metals and semiconductors contains two contributions, namely from phonon drag S_{drag} and charge carrier diffusion S_{diff} . Large thermopower values exceeding 1 000 $\mu\text{V/K}$ and in some cases even 100 000 $\mu\text{V/K}$ are usually caused by the phonon drag effect due to momentum transfer from phonons to charge carriers via electron-phonon coupling [3], e.g. in TiO_2 (200 000 $\mu\text{V/K}$) [4, 5] and $\text{Dy}_{1-x}\text{Sr}_x\text{MnO}_3$ (220 000 $\mu\text{V/K}$) [6]. However, the related good thermal conductivity is detrimental to high values of zT and applications. By contrast, the diffusion thermopower S_{diff} is typically much smaller, being of the order of 10 $\mu\text{V/K}$ for metals and a few 100 $\mu\text{V/K}$ for semiconductors below room temperature [7]. In a simple picture, it arises from a change of the number and velocity of the mobile charge carriers with temperature T due to the energy dependence of the density of states and the T dependence of the Fermi distribution [8]. The resulting imbalance in the presence of a temperature gradient ∇T leads to diffusion of

charge carriers and development of an internal electrical field E limited by a reverse ohmic current $j = \sigma E$.

Within the semiclassical Boltzman picture, the thermopower of metals and degenerate semiconductors is given by the Mott expression:

$$S_{\text{diff}} = \frac{\pi^2 k_{\text{B}}^2 T}{3q} \left(\frac{d \ln \sigma(\varepsilon)}{d\varepsilon} \right)_{E_{\text{F}}} \quad (1)$$

This equation relates S_{diff} to the logarithmic energy derivative of the conductivity $\sigma(\varepsilon)$ at the Fermi level E_{F} . k_{B} denotes the Boltzmann constant and q the charge of the carriers including sign. Equation 1 has the drawback that $\sigma(\varepsilon)$ is not directly accessible by experiments. Therefore, it is often further simplified to estimate the magnitude and temperature dependence of S . For simple metals, which can be described as a free electron gas with an energy-independent relaxation time, the derivative of equation 1 is of the order of $1/E_{\text{F}}$ [9]. This yields a linear T dependence $S \propto T/E_{\text{F}}$ with small absolute values due to the large Fermi energy in normal metals [10, 11]. By contrast, the thermopower of non-degenerate semiconductors exhibits an inverse temperature proportionality $S \propto E_{\text{g}}/T$ with the gap width E_{g} [12].

These simple concepts cannot be applied to materials with a strong temperature dependence of their electronic properties as for instance charge carrier density, chemical potential, valence, or mobility. In such a situation, any temperature gradient is accompanied by non-negligible gradients of the electronic properties of the material. In this manuscript we demonstrate how this can give rise to giant thermopower values by presenting both experimental results and a simple model taking into account such secondary gradients. In fact, it has been shown previously that a shift of the chemical potential with T related to a strongly T -dependent valence gives rise to an additional thermopower contribution in the intermediate-valence materials EuIr_2Si_2 and EuNi_2P_2 [13]. Similarly, the rapidly changing charge carrier mobility with T in $\text{Co}_{0.999}\text{Ni}_{0.001}\text{Sb}_3$ goes along with a considerable enhancement of $S(T)$ [8]. However, in both cases the overall effects have been moderate, leading to absolute thermopower values of at most 50 $\mu\text{V/K}$ and 300 $\mu\text{V/K}$, respectively. Here, we investigate $S(T)$ of EuCd_2P_2 , a material with a huge temperature and magnetic field dependence of its electrical resistivity ρ at low T suggesting dramatic changes of the charge carrier mobility and/or number of free charge carriers. In the same regime we observe giant thermopower values in zero magnetic field exceeding those of the above mentioned examples by a factor of more than 10. They can be related directly to $\rho(T)$ based on a simple drift-diffusion picture. Our findings open a new route to giant thermopower values by using gradients of electronic properties.

The investigated material EuCd_2P_2 belongs to a group of trigonal 122 compounds with CaAl_2Si_2 structure (space group $P\bar{3}m1$) that have been studied in the past as potential thermoelectrics [14–18]. More recently, this class of materials – in particular with composition $\text{Eu}T_2\text{Pn}_2$ containing transition metals $T = \text{Cd, Zn}$ and pnictides $Pn = \text{P, As, Sb}$ – arouse considerable interest due to the discovery of unconventional electronic and transport properties related to the interplay of band structure topology and magnetism [19]. The most prominent representative is EuCd_2As_2 usually classified as a topological Weyl-semimetal [20]. Recently, the material has been also suggested as a rare example to host a three dimensional van-Hove singularity [21]. Other members of the family exhibit a colossal magnetoresistance (CMR) effect, e.g. EuZn_2P_2 [22], EuZn_2As_2 under pressure [23], and the hereinafter investigated material, EuCd_2P_2 [24].

Magnetism in EuCd_2P_2 arises from Eu^{2+} moments that order antiferromagnetically at about $T_N = 11$ K [24–26]. The electrical resistivity exhibits a considerable sample dependence with semiconducting or weakly metallic behavior above about 50 K and a moderate anisotropy for the current within and perpendicular to the ab plane [24, 26]. The band structure of EuCd_2P_2 has a gap at the Fermi level as determined consistently by angle-resolved photo-emission spectroscopy (ARPES) experiments [26, 27] and band structure calculations [26, 28]. Independent of the behavior at higher T , a pronounced maximum in $\rho(T)$ is observed between about 10 K and 25 K in zero magnetic field with the resistivity changing by more than one order of magnitude. A moderate magnetic field $B = \mu_0 H$ of 1 T is sufficient to suppress the resistivity at the maximum by more than two orders of magnitude with some dependency on crystal quality and growth conditions [24, 26, 27]. The origin of the resistance maximum and CMR effect is a subject of ongoing discussions. It has been shown, that ferromagnetic interactions play an important role [29] and slight modifications in the growth conditions induce a ferromagnetic ground state via charge carrier doping [28]. The most likely scenario appears to be formation and percolation of magnetic polarons [30].

Our interest in EuCd_2P_2 arises from its huge resistivity maximum and CMR effect between about 10 K and 25 K. As explained above, the dramatic change of charge carrier transport with temperature is expected to show up also in the thermopower. Moreover, the rapid suppression of the resistivity maximum of EuCd_2P_2 in relatively small magnetic fields below 1 T allows for a direct comparison to a situation with moderate T dependence of ρ . Thus, EuCd_2P_2 with its huge temperature and field dependence of ρ appeared an ideal candidate to study the relation between electrical conductivity $\sigma = 1/\rho$ and thermopower in a situation with an extreme T dependence of

the electrical transport properties.

I. RESULTS AND DISCUSSION

A. Temperature and field dependence of the thermopower

The thermopower $S(T)$ of EuCd_2P_2 is plotted in Fig. 1a on a logarithmic temperature scale. The inset of Fig. 1a shows the data above 25 K on a linear T scale. In this region EuCd_2P_2 has a positive thermopower with relatively weak temperature dependence. This is in line with hole-like charge carriers as inferred from Hall effect measurements [28, 29], ARPES [27], and band structure calculations [26, 28]. Below 25 K the thermopower behavior changes dramatically: In a very narrow temperature region between 10 K and 20 K $S(T)$ assumes huge absolute values and switches sign twice. Below 10 K the weak temperature dependence of $S(T)$ with positive values is recovered. Fig. 1b shows the electrical resistivity measured on the same sample and contacts for comparison. In zero magnetic field $\rho(T)$ changes overall by more than four orders of magnitude and exhibits the characteristic maximum around 15 K observed on antiferromagnetic EuCd_2P_2 samples [24, 26, 28]. The maximum is dramatically suppressed in a relatively small magnetic field of 1 T.

The region between 8 K and 22 K is expanded in Fig. 2a. It shows $S(T)$ in zero magnetic field and in magnetic fields $B = \mu_0 H$ up to 1 T. In this plot one can trace the giant changes of the thermopower of EuCd_2P_2 in zero field, which to our knowledge are so far unprecedented concerning the combination of magnitude, sign changes, and extremely narrow T range: Starting from moderate positive values at 10 K the thermopower changes sign upon heating around 10.7 K, goes through a huge minimum at about 12.3 K, switches back to positive values around 13.6 K, reaches a maximum at 15.4 K, and slowly decreases towards higher T . That is, in a T range of less than 5 K the thermopower changes sign twice and alters overall by more than 4 000 $\mu\text{V/K}$. The giant slope of $S(T)$ necessitates special measurement conditions as for instance an extremely small temperature difference ΔT along the sample with $\Delta T/T < 0.12\%$ to determine the intrinsic behavior. In addition, the behavior of $S(T)$ has been confirmed on a second sample from a different batch. The respective data are shown in the supplementary information.

Application of magnetic fields leads to a rapid suppression of the huge thermopower anomaly between 10 K and 20 K, c.f. Fig. 2a. The strong field dependence is also seen in B sweeps shown

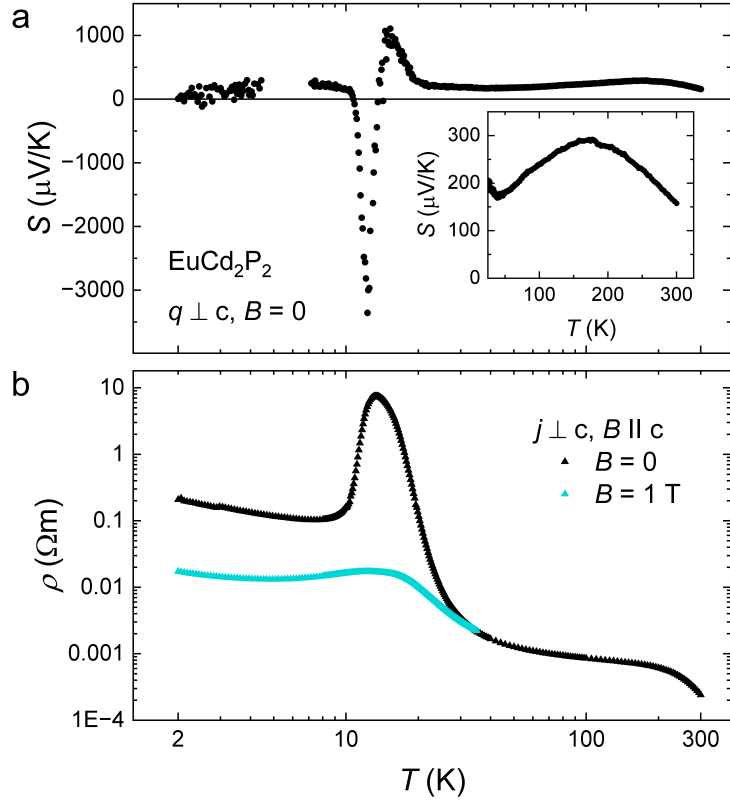


FIG. 1. **Comparison of thermopower and resistivity of EuCd_2P_2 .** **a** Thermopower S in the full investigated temperature range from 2 K to 300 K. The inset shows the high- T part of $S(T)$ on a larger scale. **b** Electrical resistivity $\rho(T)$ measured on the same sample and contacts in zero magnetic field and $B = \mu_0 H = 1$ T.

in Fig. 2b. A field of about 0.3 T is sufficient to eliminate negative thermopower values. In 0.5 T, the anomaly has disappeared completely and the thermopower remains positive without significant T dependence.

Large thermopower values are frequently associated to phonon drag. However, the complex behaviour of the thermopower anomaly of EuCd_2P_2 with two sign changes in an extremely narrow T range appears not compatible with dominating phonon drag, although the effect may play some role. We would like to explain this a little more in depth: The drag and diffusion contributions to the thermopower, S_{drag} and S_{diff} , arise from the very same charge carriers, but via two different mechanisms. S_{diff} is due to thermal diffusion of the carriers, typically from the hot to the cold end of the sample. In addition, these charge carriers are dragged along by phonons, also usually towards the cold side. Therefore, in simple materials with carriers of a single polarity, both con-

tributions have the same sign leading to a positive thermopower for hole-like charge carriers and a negative one for electrons. A sign change in $S(T)$ as observed for EuCd_2P_2 could then be caused by a change of the dominating type of charge carriers. This would also imply a polarity reversal of S_{drag} . However, there is no indication for such an effect in EuCd_2P_2 neither from ARPES nor band structure calculations, while the Hall effect is dominated by an anomalous contribution. Another mechanism, that may give rise to a change of sign in S_{drag} , is phonon-charge carrier Umklapp scattering [31]. It leads to a reversal of the charge carrier flow and may result in a sign change of S_{drag} if strong enough. This effect is largest around $\Theta_D/5$, Θ_D being the Debye temperature. It is held responsible for the sign change of $S(T)$ in various materials, e.g. PdCoO_2 [32] or doped KTaO_3 thin films [33] and might also play a role in semiconductor superlattices [34]. However, for EuCd_2P_2 the temperature of the minimum in $S(T)$ of about 12 K appears rather low compared to the estimate of $\Theta_D = 147$ K from specific heat [26]. Most important, to the best of our knowledge there is no single mechanism that gives rise to two sign changes in S_{drag} . The only conceivable situations would be a combination of effects or switching the carrier type twice. This appears highly unlikely and practically rules out phonon drag as the main origin for the rather complex anomaly in $S(T)$.

Before discussing an alternative scenario for the unusual thermopower of EuCd_2P_2 we would like to rank the observed values and field dependence. In literature the terms "giant" or "colossal" thermopower have been used for a wide range of absolute values. Some of the largest thermopowers in bulk materials have been observed in manganates as $\text{Dy}_{1-x}\text{Sr}_x\text{MnO}_3$ (220 000 $\mu\text{V/K}$) [6] and $\text{Gd}_{1-x}\text{Sr}_x\text{MnO}_3$ (35 000 $\mu\text{V/K}$) [35], in TiO_2 (200 000 $\mu\text{V/K}$) [4], and in FeSb_2 (45 000 $\mu\text{V/K}$) [36]. However, as mentioned in our introduction the thermopower in these systems is at least to some extend enhanced by phonon drag [5, 6, 37]. By contrast, the diffusion thermopower in metals and semiconductors is typically three orders of magnitude lower with values of 10-100 $\mu\text{V/K}$ [7]. Based on this scale, the thermopower of 400 $\mu\text{V/K}$ observed in the clathrate system $\text{Ba}_8(\text{Cu},\text{Zn})_x\text{Ge}_{46-x}$ has also been labeled as "giant" [38]. The observation of absolute values exceeding 3 000 $\mu\text{V/K}$ in EuCd_2P_2 is therefore clearly remarkable.

Besides the large absolute values of S observed in EuCd_2P_2 in zero magnetic field, the dramatic suppression in relatively small magnetic fields is also remarkable. Typically "giant" magnetothermopower values defined as $|S(B) - S(0)|$ are claimed for applied fields of several tesla. Some examples are summarized in table I in comparison to EuCd_2P_2 . Besides the maximum change of S in magnetic fields, also the steepest slope $|\text{d}S/\text{d}B|_{\text{max}}$ is given. The values in table I demon-

TABLE I. Materials claimed to exhibit a giant magnetothermopower. The maximum reported value $dS_{\max} = |S(B) - S(0)|$ is given together with the corresponding temperature T_{\max} and magnetic field B_{\max} . In addition, the steepest slope $|dS/dB|_{\max}$ is specified.

Material	dS_{\max} [$\mu\text{V/K}$]	$T(S_{\max})$ [K]	$B(S_{\max})$ [T]	$ dS/dB _{\max}$ [$\mu\text{V/KT}$]	reference
EuCd_2P_2	3 600	12	0.5	13 000	this study
InAs	10 000	8	29	800	[39]
Bi	4 000	7	5	1 500	[40]
NbP	800	50	9	150	[41]
$\text{Ag}_{2-\delta}\text{Te}$	470	110	7	150	[42]

strate that EuCd_2P_2 is indeed exceptional, both concerning the low field required to induce a large magnetothermopower and the huge slope of $S(B)$. Interestingly, the absolute values of $S(T)$ of EuCd_2P_2 decrease with increasing magnetic field, while all other materials mentioned in table I exhibit an opposite field dependence.

Summing up, the thermopower of EuCd_2P_2 in the T range of 10-20 K is highly unconventional with respect to four facts: (1) huge absolute values primarily not due to phonon drag, (2) an extremely strong temperature dependence with the slope exceeding $2\,000\,\mu\text{V/K}^2$, (3) a dramatic suppression of S in exceptionally small magnetic fields, and (4) an overall unusual T dependence with two sign changes within 3 K.

B. Relation between thermopower and resistivity

As discussed above, the thermopower anomaly of EuCd_2P_2 cannot be caused by phonon drag, at least not exclusively. Therefore, we have to search for an alternative explanation. Comparing the thermopower to the electrical resistivity reveals that both properties exhibit highly unconventional behavior in a similar temperature and field range. However, the sensitivity of the thermopower to field is even stronger: The anomaly of $S(T)$ is located between 10 and 20 K and fully suppressed by a field of about 0.3 T. By contrast, the huge maximum in $\rho(T)$ is still visible in a field of 1 T, cf. Fig. 1b, although it is much broader and smaller than in zero field. Nevertheless, it appears most natural that both effects should be related: The giant T dependence of the electrical resistivity in

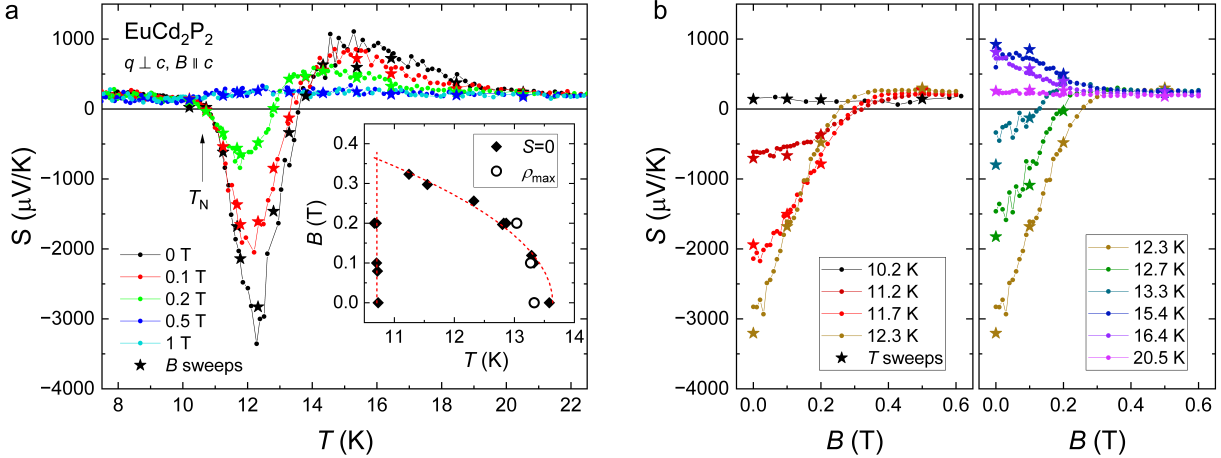


FIG. 2. Thermopower of EuCd_2P_2 in magnetic fields. **a** Temperature dependence of the thermopower S of EuCd_2P_2 at different magnetic fields $B = \mu_0 H$. The anomaly is rapidly suppressed by small fields. The results from T sweeps (lines with small symbols) are in good agreement with those from B sweeps (asterisks). The Néel temperature T_N in zero field is marked by an arrow. The inset shows the position of the maxima in $\rho(T)$ and of sign changes in $S(T)$ and $S(B)$. The lines are guides to the eye. **b** Field dependence of the thermoelectric power S of EuCd_2P_2 at different temperatures. B sweeps (lines with small symbols) and T sweeps (asterisks) exhibit the same behavior.

EuCd_2P_2 – changing for instance by more than an order of magnitude upon cooling from 20 K to 15 K – leads to a sizeable resistivity gradient in the presence of a temperature gradient. This in turn is expected to have an impact on the thermopower. Consistently, the maximum in $\rho(T)$ at 13.5 K coincides with a sign change and, therefore, also small values of $S(T)$. This is demonstrated in the inset of Fig. 2a. It shows the positions of the maxima in $\rho(T)$ and where $S = 0$. The second sign change in $S(T)$ at lower T occurs close to the ordering temperature T_N , which is 10.6 K for our samples in zero field and has an only weak field dependence up to 0.4 T [26].

These observations raise the question, how the strong T dependence of the resistivity influences the diffusion contribution to the thermopower. In fact, S_{diff} of EuCd_2P_2 cannot be understood from simple diffusion pictures for normal metals or semiconductors. The widely-used Mott relation is only applicable to systems with a Fermi surface or finite density of states at the Fermi level as metals or heavily-doped semiconductors. However, it has been shown by ARPES and band structure calculations that EuCd_2P_2 has a gap at the Fermi level [26–28]. On the other hand, the material also cannot be treated as a conventional non-degenerate semiconductor, at least not in the T range

of interest. The large maximum in the electrical resistivity below 30 K clearly demonstrates that any picture based on activation via a constant band gap or hopping barrier is inapplicable in this regime. Most important, the huge resistivity gradient induced by ∇T needs to be included in any thermopower model for EuCd_2P_2 : For example, around 11 K, i.e. close to the largest slope of $\rho(T)$ a temperature difference of 1 % gives rise to more than 20 % change in resistivity. This effect is much stronger than, e.g., thermal broadening of the Fermi-Dirac distribution, which is the main source for the thermopower in simple models as the Mott relation.

In order to evaluate the relation between the thermopower and resistivity anomalies of EuCd_2P_2 , we start from a macroscopic transport picture. At this point, we are only interested in the impact of the strong changes in $\rho(T)$ on S_{diff} . The material is treated as being single phase with homogeneous properties apart from its strongly T -dependent electrical transport. That is, we do not consider local inhomogeneities arising from ferromagnetic-cluster or magnetic-polaron formation. In this picture the thermopower results from a balance between two currents: a diffusion current j_{diff} due to a change of electronic and transport properties with T and a drift current j_{drift} arising from the developing electrical field E . In our evaluation of the thermopower we allow explicitly for a variation in the charge carrier density n and diffusion coefficient D along the sample. The latter is usually assumed constant or quasi-constant in literature, which is an important difference to our calculation. The situation with variable n and D is described by the Stratton equation [43]. The total electrical current along a specific direction (e.g. x) amounts to

$$j_x = j_{\text{diff}} + j_{\text{drift}} = \sigma E_x - q \frac{\partial(nD)}{\partial x} \quad (2)$$

For simplicity we ignore anisotropies of transport coefficients and omit the corresponding subscripts. In thermopower measurements, the net current is zero and the diffusion and drift currents have opposite direction: $j_{\text{diff}} = -j_{\text{drift}}$. Assuming a constant temperature gradient along the sample we may replace the derivative with respect to x by the one with respect to T : $\partial(nD)/\partial x = \partial(nD)/\partial T \cdot \nabla T$. In addition we use the relations between diffusion coefficient D , mobility μ , and electrical conductivity σ to replace $D = \mu k_B T / q$ by $\sigma = n \mu q$, with the Boltzmann constant k_B . Thus, we get a direct relation between the diffusion thermopower and electrical conductivity:

$$S_{\text{diff}} = \frac{E}{\nabla T} = \frac{k_B}{q} \frac{1}{\sigma} \frac{\partial(\sigma T)}{\partial T} = \frac{k_B}{q} \left(1 + \frac{\partial \ln \sigma}{\partial \ln T} \right) \quad (3)$$

In a trigonal system as EuCd_2P_2 , electrical conductivity and resistivity along high-symmetry directions are directly inverse, i.e., for j along [210] we can take $\sigma = 1/\rho$. Therefore, equation

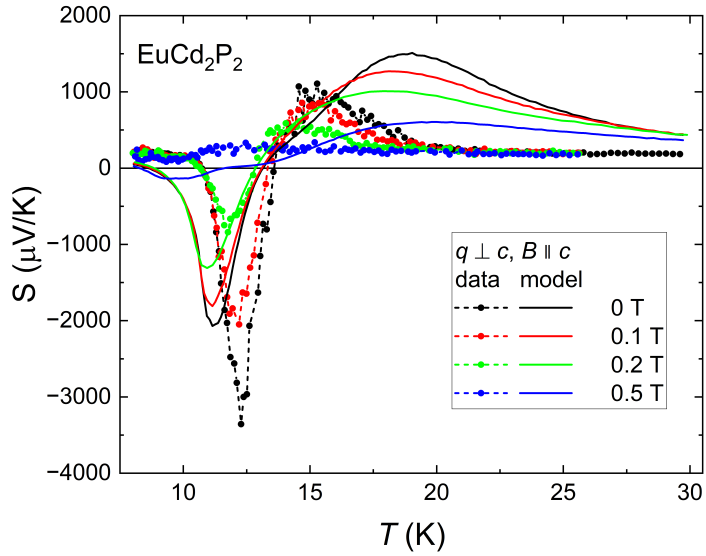


FIG. 3. **Drift-diffusion model of the thermopower.** Temperature dependence of the thermoelectric power S of EuCd_2P_2 at different magnetic fields. Lines are calculations from the electrical resistivity based on a parameter-free drift-diffusion model as explained in the main text.

3 allows a calculation of the diffusion thermopower from the electrical resistivity. The results obtained for EuCd_2P_2 and hole-like charge carriers are plotted in Fig. 3. The resemblance of calculation and data is extremely good taking into account the simplicity of our assumptions. In fact, equation 3 predicts the correct shape, sign, magnitude, and field dependence of the thermopower. The main difference is the width of the anomalies in $S(T)$. The strongest temperature dependence is observed in a more narrow regime than predicted by equation 3. These deviations can be attributed to the simplicity of our drift-diffusion picture of classical particles, which does not account for impact from different scattering or transport channels, local inhomogeneities due to ferromagnetic domain or polaron formation, percolation effects, and variations in the chemical potential with T . The relevance of these factors might be evaluated by systematically studying the thermopower of crystals grown under different conditions. In fact, it has been shown, that small variations in the charge carrier concentration may lead to dramatic changes in the magnetic and transport properties of the material [28]. Moreover, we cannot exclude that phonon drag plays a certain role in the material and gives rise to an additional contribution to $S(T)$.

Altogether, our very simple model is able to account for all four of the above-mentioned aspects of the highly unconventional thermopower of EuCd_2P_2 . In particular we would like to emphasize that there is no free parameter in our calculation: The only ingredients are the electrical resistivity

and the charge carrier type, while the microscopic origin of the strong T dependence of $\rho(T)$ and the CMR are not considered. Therefore, the similarity between the calculated and measured thermopower curves is indeed impressive. It clearly demonstrates, that the unusual temperature and field dependencies of S in EuCd_2P_2 are caused by the strong changes of the electrical resistivity with T and B .

Despite the large thermopower observed in EuCd_2P_2 , the thermoelectric figure of merit zT is very small – about 10^{-7} at 12 K. This is mainly due to the extremely high electrical resistivity of the material. In general, usage of the presented effect in thermoelectric devices is limited by the small temperature region of the thermopower enhancement. It is directly related to the strong T dependence of the electrical resistivity, which cannot be perpetuated over a large T range. This drawback might be overcome to some extend by material's customization to operating environments. Independent of these limitations, our finding proofs the direct relation between thermopower and resistivity anomalies in EuCd_2P_2 . This shows that in general, it is possible to generate a large thermopower as needed for decent zT values via secondary gradients of electronic properties. A possible direction for exploitation of this mechanism is the search for materials with secondary gradients of other electronic properties or the use of internal compositional gradients induced via position-dependent doping.

II. METHODS

Thermal and electrical transport measurements were performed on single crystals of EuCd_2P_2 grown from Sn flux [26]. The crystals grow as plates with the short dimension along [001]. They were cut to bars with the long extension along [210]. Four micro-contacts were sputtered onto the sample consisting of a 10 nm titanium layer covered by a 150 nm gold layer. Typical sample dimensions were $3 \times 1 \times 0.5 \text{ mm}^3$ with the distance between the middle contacts being about 1.5 mm.

Thermoelectric transport measurements were performed in a commercial Physical Property Measurement System (PPMS) from Quantum Design (QD) using the thermal transport option (TTO). For this purpose, Au-coated Cu bars were attached with silver paint to the microcontacts. The TTO allows measurement of thermal conductivity, thermoelectric power, and AC electrical resistivity in a single run and using the same contacts. However, in order to avoid sample heating and long relaxation times between thermal measurements, we performed resistivity measurement

in separate runs.

The thermal conductivity κ and thermopower S were measured using a standard steady-state method with a two-thermometer-one-heater configuration in the T range of 2 K - 300 K. The heat current j_Q was applied along [210] and the magnetic field along [001]. For temperature-dependent measurements, square-wave heat pulses were applied and the time evolution of temperature difference and voltage along the sample monitored, while continuously sweeping the bath temperature. The thermal conductivity and thermopower were then calculated by a fitting routine, which also estimates the adequate power and duration for the next heat pulse. Magnetic-field-dependent measurements were performed at constant bath temperature and field using a constant heater power. Due to the negligible field-dependence of the thermal conductivity, it is assumed that measurements effectively take place at constant average sample T . Several data points were taken at each field to allow for averaging before sweeping to the next set point. In addition, continuous measurements were performed while sweeping the field in regimes with very weak field-dependence. These measurements are much faster. However, data spacing is much larger due to the minimum sweep rate of the magnet.

The TTO measures the electrical resistivity ρ using a 4-point AC technique. However, ρ could not be resolved at low T and B probably because of sample self heating. Therefore, we performed additional measurements using the AC transport option (ACTO) of the PPMS and a low excitation current of 0.01 mA. For this purpose, we attached Au wires to the same micro-contacts used for thermoelectric transport measurements. The sample had a large contact area to the bath, and measurements were performed in He atmosphere for thermalization. Both methods, TTO and ACTO, are in good agreement confirming the equal geometry factor and the quality of our thermal transport contacts. The results are shown in the supplementary information.

In the T range between 10 K and 20 K, extremely large values of ρ and a giant T dependence of both ρ and S are observed in EuCd₂P₂. For instance, changing the temperature from 11.5 K to 11.6 K, i.e. by less than 1 %, leads to an increase of ρ by 22 %. In the same T range, S changes by about 260 μ V/K corresponding to 17 % at this temperature. In order to ensure reliability of our data, we took several precautions:

- The dramatic temperature dependence of S requires measurements at very low T gradient to establish a quasi-constant situation along the sample. Below 20 K we applied an extremely small T difference ΔT along the sample with $\Delta T/T < 0.12 \%$. This tiny gradient is

responsible for the enhanced noise at low T in our data.

- We confirmed that our results from T sweeps and B sweeps are consistent. This is important, because the T dependent thermopower was measured while sweeping the bath temperature. The agreement with results from field sweeps validates, that the sweep rate of 0.1 K/min was sufficiently low.
- In addition, we confirmed that S is roughly independent of the applied temperature gradient by measuring exemplarily field sweeps at 11.5 K for two different values of ΔT , namely 5 mK and 7.5 mK. The resulting thermopower curves can be scaled by a factor of 1.1, which is small compared to the observed field and temperature dependencies.

- [1] Doug Crane, Bed Poudel, Wenjie Li, and Giri Joshi. Thermoelectric applications, innovations, and impact across industries. *MRS Bulletin*, 50:902, 2025.
- [2] Kefeng Wang, Limin Wang, and C. Petrovic. Large magnetothermopower effect in Dirac materials $(\text{Sr/Ca})\text{MnBi}_2$. *Appl. Phys. Lett.*, 100(11):112111, 03 2012.
- [3] J. M. Ziman. *Electrons and Phonons: The Theory of Transport Phenomena in Solids*. Oxford University Press, New York, 2001.
- [4] W. R. Thurber and A. J. H. Mante. Thermal conductivity and thermoelectric power of rutile (TiO_2). *Phys. Rev.*, 139:A1655–A1665, Aug 1965.
- [5] Jinke Tang, Wendong Wang, Guang-Lin Zhao, and Qiang Li. Colossal positive Seebeck coefficient and low thermal conductivity in reduced TiO_2 . *J. Phys.: Cond. Matter*, 21(20):205703, apr 2009.
- [6] B. S. Nagaraja, Ashok Rao, and G. S. Okram. Structural, electrical, and colossal thermoelectric properties of $\text{Dy}_{1-x}\text{Sr}_x\text{MnO}_3$ manganites. *J. Supercond. Nov. Magn.*, 28:223, 2015.
- [7] H. Julian Goldsmid. *Introduction to Thermoelectricity*. Springer Series in Materials Science Vol. 121, Springer-Verlag Berlin, 2010.
- [8] P. Sun, B. Wei, J. Zhang, J. M. Tomaczak, A. M. Strydom, M. Sondergaard, B. B. Iversen, and F. Steglich. Large Seebeck effect by charge-mobility engineering. *Nat. Commun.*, 6:7475, 2015.
- [9] S. Paschen. *Thermoelectric aspects of strongly correlated electron systems*. Thermoelectrics handbook: macro to nano (Chapter 15). D. M. Rowe, ed., CRC Press, Taylor & Francis Group, Boca Raton, FL, 2006.

[10] Kamran Behnia, Didier Jaccard, and Jacques Flouquet. On the thermoelectricity of correlated electrons in the zero-temperature limit. *Journal of Physics: Condensed Matter*, 16(28):5187, jul 2004.

[11] A. Akrap, N. Barišić, L. Forró, D. Mandrus, and B. C. Sales. High-pressure resistivity and thermoelectric power in $\text{Yb}_{14}\text{MnSb}_{11}$. *Phys. Rev. B*, 76:085203, 2007.

[12] A. P. Gonçalves and C. Godart. Alternative strategies for thermoelectric materials development. In Veljko Zlatić and Alex Hewson, editors, *New Materials for Thermoelectric Applications: Theory and Experiment*, pages 1–24, Dordrecht, 2013. Springer Netherlands.

[13] U. Stockert, S. Seiro, N. Caroca-Canales, E. Hassinger, and C. Geibel. Valence effect on the thermopower of Eu systems. *Phys. Rev. B*, 101:235106, Jun 2020.

[14] A. Artmann, A. Mewis, M. Roepke, and G. Michels. AM_2X_2 -Verbindungen mit CaAl_2Si_2 -Struktur. XI. Struktur und Eigenschaften der Verbindungen ACd_2X_2 (A: Eu, Yb; X: P, As, Sb). *Z. Anorg. Allg. Chem.*, 622(4):679–682, 1996.

[15] Hui Zhang, Jing-Tai Zhao, Yu. Grin, Xiao-Jun Wang, Mei-Bo Tang, Zhen-Yong Man, Hao-Hong Chen, and Xin-Xin Yang. A new type of thermoelectric material, EuZn_2Sb_2 . *J. Chem. Phys.*, 129(16):164713, 10 2008.

[16] Hui Zhang, Liang Fang, Mei-Bo Tang, Hao-Hong Chen, Xin-Xin Yang, Xiangxin Guo, Jing-Tai Zhao, and Yuri Grin. Synthesis and properties of CaCd_2Sb_2 and EuCd_2Sb_2 . *Intermetallics*, 18(1):193–198, 2010.

[17] Andrew F. May, Michael A. McGuire, David J. Singh, Jie Ma, Olivier Delaire, Ashfia Huq, Wei Cai, and Hsin Wang. Thermoelectric transport properties of CaMg_2Bi_2 , EuMg_2Bi_2 , and YbMg_2Bi_2 . *Phys. Rev. B*, 85:035202, Jan 2012.

[18] T. Wubieneh, P. Wei, C. Yeh, S. Chen, and Y. Chen. Thermoelectric properties of Zintl phase compounds of $\text{Ca}_{1-x}\text{Eu}_x\text{Zn}_2\text{Sb}_2$ ($0 \leq x \leq 1$). *J. Electron. Mater.*, 45:1942, 2015.

[19] Kristin Kliemt. Chemical pressure due to impurities in trigonal compounds EuT_2Pn_2 (T= Cd, Zn; Pn= P, As, Sb). *Progr. Cryst. Growth Charact. Mater.*, 71(2):100667, 2025.

[20] J.-Z. Ma, S. M. Nie, C. J. Yi, J. Jandke, T. Shang, M. Y. Yao, M. Naamneh, L. Q. Yan, Y. Sun, A. Chikina, V. N. Strocov, M. Medarde, M. Song, Y.-M. Xiong, G. Xu, W. Wulfhekel, J. Mesot, M. Reticcioli, C. Franchini, C. Mudry, M. Müller, Y. G. Shi, T. Qian, H. Ding, and M. Shi. Spin fluctuation induced Weyl semimetal state in the paramagnetic phase of EuCd_2As_2 . *Sci. Adv.*, 5(7):eaaw4718, 2019.

[21] Wenbin Wu, Zeping Shi, Mykhaylo Ozerov, Yuhan Du, Yuxiang Wang, Xiao-Sheng Ni, Xianghao Meng, Xiangyu Jiang, Guangyi Wang, Congming Hao, Xinyi Wang, Pengcheng Zhang, Chunhui Pan,

Haifeng Pan, Zhenrong Sun, Run Yang, Yang Xu, Yusheng Hou, Zhongbo Yan, Cheng Zhang, Junhao Chu, and Xiang Yuan. The discovery of three-dimensional Van Hove singularity. *Nat. Commun.*, 15:2313, 2024.

[22] Sarah Krebber, Marvin Kopp, Charu Garg, Kurt Kummer, Jörg Sichelschmidt, Susanne Schulz, Georg Poelchen, Max Mende, Alexander V. Virovets, Konstantin Warawa, Mark D. Thomson, Artem V. Tarasov, Dmitry Yu. Usachov, Denis V. Vyalikh, Hartmut G. Roskos, Jens Müller, Cornelius Krellner, and Kristin Kliemt. Colossal magnetoresistance in EuZn_2P_2 and its electronic and magnetic structure. *Phys. Rev. B*, 108:045116, Jul 2023.

[23] Shuaishuai Luo, Yongkang Xu, Feng Du, Lin Yang, Yuxin Chen, Chao Cao, Yu Song, and Huiqiu Yuan. Colossal magnetoresistance and topological phase transition in EuZn_2As_2 . *Phys. Rev. B*, 108:205140, Nov 2023.

[24] Zhi-Cheng Wang, Jared D. Rogers, Xiaohan Yao, Renee Nichols, Kemal Atay, Bochao Xu, Jacob Franklin, Ilya Sochnikov, Philip J. Ryan, Daniel Haskel, and Fazel Tafti. Colossal magnetoresistance without mixed valence in a layered phosphide crystal. *Adv. Mater.*, 33(10):2005755, 2021.

[25] Inga Schellenberg, Ulrike Pfannenschmidt, Matthias Eul, Christian Schwickert, and Rainer Pöttgen. A ^{121}Sb and ^{151}Eu Mössbauer spectroscopic investigation of EuCd_2X_2 ($\text{X} = \text{P}, \text{As}, \text{Sb}$) and YbCd_2Sb_2 . *Z. Anorg. Allg. Chem.*, 637(12):1863–1870, 2011.

[26] Dmitry Yu. Usachov, Sarah Krebber, Kirill A. Bokai, Artem V. Tarasov, Marvin Kopp, Charu Garg, Alexander Virovets, Jens Müller, Max Mende, Georg Poelchen, Denis V. Vyalikh, Cornelius Krellner, and Kristin Kliemt. Magnetism, heat capacity, and electronic structure of EuCd_2P_2 in view of its colossal magnetoresistance. *Phys. Rev. B*, 109:104421, Mar 2024.

[27] Huali Zhang, Feng Du, Xiaoying Zheng, Shuaishuai Luo, Yi Wu, Hao Zheng, Shengtao Cui, Zhe Sun, Zhengtai Liu, Dawei Shen, Michael Smidman, Yu Song, Ming Shi, Zhicheng Zhong, Chao Cao, Huiqiu Yuan, and Yang Liu. Electronic band reconstruction across the insulator-metal transition in colossally magnetoresistive EuCd_2P_2 . *Phys. Rev. B*, 108:L241115, Dec 2023.

[28] Xiyu Chen, Ziwen Wang, Zhiyu Zhou, Wuzhang Yang, Yi Liu, Jia-Yi Lu, Zhi Ren, Guang-Han Cao, Fazel Tafti, Shuai Dong, and Zhi-Cheng Wang. Manipulating magnetism and transport properties of EuCd_2P_2 with a low carrier concentration. *Phys. Rev. B*, 109:224428, Jun 2024.

[29] V. Sunko, Y. Sun, M. Vranas, C. C. Homes, C. Lee, E. Donoway, Z.-C. Wang, S. Balguri, M. B. Mahendru, A. Ruiz, B. Gunn, R. Basak, S. Blanco-Canosa, E. Schierle, E. Weschke, F. Tafti, A. Frano, and J. Orenstein. Spin-carrier coupling induced ferromagnetism and giant resistivity peak in EuCd_2P_2 .

Phys. Rev. B, 107:144404, Apr 2023.

- [30] Marvin Kopp, Charu Garg, Sarah Krebber, Kristin Kliemt, Cornelius Krellner, Sudhaman Balguri, Mira Mahendru, Fazel Tafti, Theodore L. Breeze, Nathan P. Bentley, Francis L. Pratt, Thomas J. Hicken, Hubertus Luetkens, Jonas A. Krieger, Stephen J. Blundell, Tom Lancaster, M. Victoria Ale Crivillero, Steffen Wirth, and Jens Müller. Robust magnetic polaron percolation in the anti-ferromagnetic CMR system EuCd₂P₂. npj Quantum Mater., 2026.
- [31] K. D. Belashchenko and D. V. Livanov. Phonon effects in the thermoelectric power of impure metals. Journal of Physics: Condensed Matter, 10(34):7553, Aug 1998.
- [32] Ramzy Daou, Raymond Frésard, Sylvie Hébert, and Antoine Maignan. Large anisotropic thermal conductivity of the intrinsically two-dimensional metallic oxide PdCoO₂. Phys. Rev. B, 91:041113, Jan 2015.
- [33] Mohamed Nawwar, Samuel Poage, Tobias Schwaigert, Maria N. Gastiasoro, Salva Salmani-Rezaie, Darrell G. Schlom, Kaveh Ahadi, Brandi L. Wooten, and Joseph P. Heremans. Large phonon-drag thermopower polarity reversal in Ba-doped KTaO₃. ArXiv, page 2508.00313v1, 2025.
- [34] S. S. Kubakaddi, P. N. Butcher, and B. G. Mulimani. Influence of umklapp processes on the sign of phonon-drag thermopower in semiconductor superlattices. Journal of Physics: Condensed Matter, 3(28):5445, jul 1991.
- [35] S. Sagar, V. Ganesan, P. A. Joy, Senoy Thomas, A. Liebig, M. Albrecht, and M. R. Anantharaman. Colossal thermoelectric power in gd-sr manganites. Europhys. Lett., 91(1):17008, jul 2010.
- [36] A. Bentien, S. Johnsen, G. K. H. Madsen, B. B. Iversen, and F. Steglich. Colossal Seebeck coefficient in strongly correlated semiconductor FeSb₂. Europhys. Lett., 80(1):17008, sep 2007.
- [37] M. Battiat, J. M. Tomczak, Z. Zhong, and K. Held. Unified picture for the colossal thermopower compound fesb₂. Phys. Rev. Lett., 114:236603, Jun 2015.
- [38] I. Bednar, E. Royanian, S. Bühler-Paschen, E. Bauer, N. Nasir, A. Grytsiv, N. Melnychenko-Koblyuk, and P. Rogl. Giant thermopower at low temperatures in novel clathrates Ba₈(Cu,Zn)_xGe_{46-x}. J. Electron. Mater., 39:1687, 2010.
- [39] Alexandre Jaoui, Gabriel Seyfarth, Carl Willem Rischau, Steffen Wiedmann, Siham Benhabib, Cyril Proust, Kamran Behnia, and Benoît Fauqué. Giant Seebeck effect across the field-induced metal-insulator transition of InAs. npj Quantum Mater., 5:94, 2020.
- [40] J. H. Mangez, J. P. Issi, and J. Heremans. Transport properties of bismuth in quantizing magnetic fields. Phys. Rev. B, 14:4381–4385, Nov 1976.

- [41] U. Stockert, R. D. dos Reis, M. O. Ajeesh, S. J. Watzman, M. Schmidt, C. Shekhar, J. P. Heremans, C. Felser, M. Baenitz, and M. Nicklas. Thermopower and thermal conductivity in the Weyl semimetal NbP. *J. Phys.: Cond. Matter*, 29(32):325701, jul 2017.
- [42] Young Sun, M. B. Salamon, M. Lee, and T. F. Rosenbaum. Giant magnetothermopower associated with large magnetoresistance in $\text{Ag}_{2-\delta}\text{Te}$. *Appl. Phys. Lett.*, 82(9):1440–1442, 03 2003.
- [43] R. Stratton. Diffusion of hot and cold electrons in semiconductor barriers. *Phys. Rev.*, 126:2002–2014, Jun 1962.

III. ACKNOWLEDGMENTS

We would like to thank B. Fauqué and K. Behnia for clarifying discussions. We acknowledge funding from the Deutsche Forschungsgemeinschaft (DFG, German Research Foundation) through the Collaborative Research Centers CRC 288 (422213477, Project No. A03) and CRC 1143 (247310070, Project No. C10) and through the Würzburg-Dresden Cluster of Excellence ctd.qmat - Complexity, Topology and Dynamics in Quantum Matter (EXC 2147, project-id 390858490). We acknowledge financial support from the Max Planck Society through the Physics of Quantum Materials department and the research group "Physics of Unconventional Metals and Superconductors (PUMAS)".

IV. SUPPLEMENTARY INFORMATION

A. Electrical resistivity of EuCd_2P_2

Fig. 4 shows a comparison of our resistivity measurements performed with the thermal transport option (TTO) and the ac transport option (ACTO) of a Physical Property Measurement System (PPMS) on the same sample and gold contacts. At high T both measurements yielded very similar results. The large resistances at low T and B could not be resolved by the TTO, probably due to sample self heating.

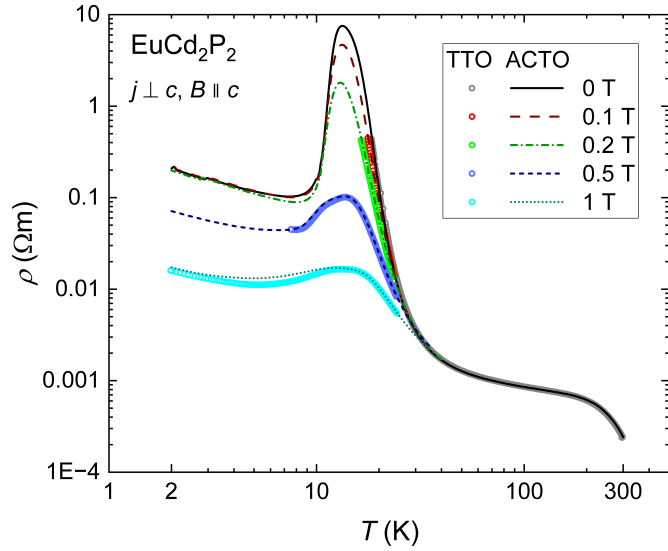


FIG. 4. **Electrical resistivity of EuCd_2P_2 .** Comparison of the electrical resistivity ρ of EuCd_2P_2 obtained on the same contacts, but with two different measurement techniques. Data points have been measured using the TTO. The lines correspond to measurements with the ACTO. Both methods yield the same results at high T and B . However, the TTO was not able to resolve very large resistances, as observed in low fields below 20 K in EuCd_2P_2 .

B. Thermal conductivity of EuCd_2P_2

Fig. 5 shows the thermal conductivity κ of EuCd_2P_2 in zero magnetic field and 1 T. The rather large noise below 20 K is due to the very small T gradient applied in this T range as explained in the methods section. In fact, in the temperature range between about 4 K and 7 K κ could not

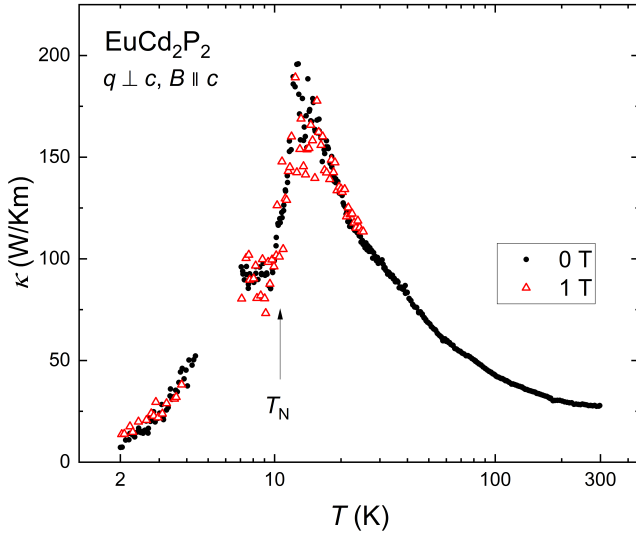


FIG. 5. **Thermal conductivity κ of EuCd_2P_2 .** Measurements in zero field and 1 T yielded very similar results indicating a negligible field dependence of κ in this region.

be resolved due to the small T gradient and large thermal conductivity of the sample. Apart from this region, EuCd_2P_2 exhibits the typical behavior of a semiconductor with a thermal conductivity due to phonons: $\kappa(T)$ initially increases with increasing T , reaches a maximum around 15 K and decreases towards higher T . The electronic contribution to the thermal conductivity estimated from the electrical resistivity using the Wiedemann-Franz law is more than six orders below the measured κ values. This clearly shows, that κ is solely due to phonons. Application of a magnetic field does not alter the thermal conductivity, which is also in line with a purely phononic κ .

C. Thermopower of a second sample

In order to confirm the observed behavior and absolute values of the thermopower of EuCd_2P_2 we studied a second sample (sample 2) from a different batch. The results are compared to those presented in the main text (sample 1) in Fig. 6. The dimensions of sample 2 were slightly shorter than for sample 1. Therefore, the corresponding measurement was more noisy, and we had problems to resolve the temperature gradient below 12 K. However, as demonstrated in Fig. 6a, both samples exhibit a very similar temperature and field dependence of the anomaly at low T . Above 25 K the thermopower curves of both samples differ slightly, cf. Fig. 6b. This may be caused by a different amount impurities acting as dopants.

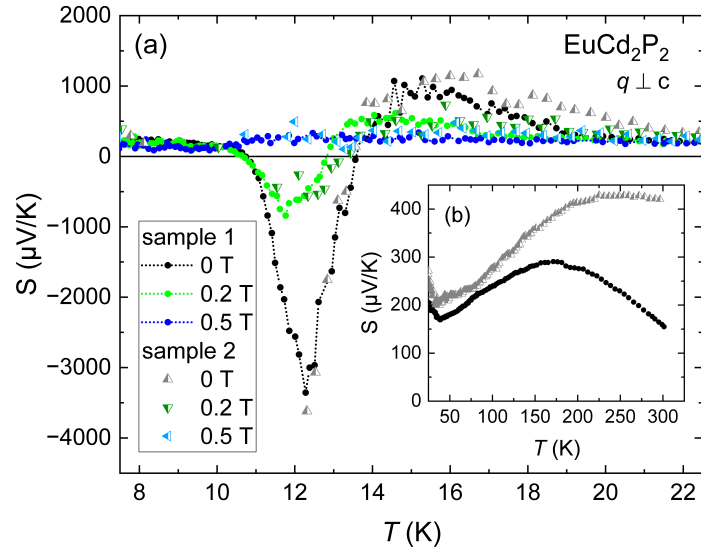


FIG. 6. **Comparison of the thermopower for two different samples of EuCd_2P_2 .** (a) Anomaly at low T in different magnetic fields. (b) Behavior of the thermopower in the regime 25 K - 300 K.